



Cite this: *J. Mater. Chem. B*, 2017, 5, 3132

Hybrid inhalable microparticles for dual controlled release of levofloxacin and DNase: physicochemical characterization and *in vivo* targeted delivery to the lungs†

G. A. Islan,^a M. E. Ruiz,^{bc} J. F. Morales,^{bc} M. L. Sbaraglini,^c A. V. Enrique,^c G. Burton,^d A. Talevi,^c L. E. Bruno-Blanch^c and G. R. Castro^{ib}*^a

Current medical treatments against recurrent pulmonary infections caused by *Pseudomonas aeruginosa*, such as cystic fibrosis (CF) disorder, involve the administration of inhalable antibiotics. The main challenge is, however, the eradication of microbial biofilms immersed in dense mucus that requires high and recurrent antibiotic doses. Accordingly, the development of novel drug delivery systems capable of providing local and controlled drug release in the lungs is a key factor to improve the therapeutic outcome of such therapeutic molecules. Inhalable hybrid carriers were prepared by co-precipitation of CaCO₃ in the presence of alginate and the resulting microparticles were treated with alginate lyase (AL) in order to modify their porosity and enhance the drug loading. The hybrid microparticles were loaded with DNase (mucolytic agent) and levofloxacin (LV, wide-spectrum antibiotic) in the range of 20–40% for LV and 28–67% for DNase, depending on the AL treatment. *In vitro* studies demonstrated that microparticles were able to control the DNase release for 24 h, while 30–50% of LV was released in 3 days. The morphological characterization was performed by optical, fluorescence and scanning electron microscopies, showing a narrow size distribution (5 μm). FTIR, XRD, DSC and nitrogen adsorption isotherm studies revealed the presence of the drugs in a non-crystalline state. A microcidal effect of microparticles was found on *P. aeruginosa* in agar plates and corroborated by Live/Dead kit and TEM observations. Finally, to study whether the microparticles improved the localization of LV in the lungs, *in vivo* studies were performed by pulmonary administration of microparticles to healthy mice *via* nebulization and dry powder inhalation, followed by the quantification of LV in lung tissue. The results showed that microparticles loaded with LV delivered the antibiotic at least 3 times more efficiently than free LV. The developed system opens the gateway to new drug delivery systems that may provide enhanced therapeutic solutions against bacterial infections and in particular as a potential tool in CF pathology.

Received 27th December 2016,
Accepted 28th March 2017

DOI: 10.1039/c6tb03366k

rsc.li/materials-b

Introduction

Cystic fibrosis (CF) is one of the most common lethal genetic human disorders, prevalent in Caucasian populations. It is attributed to the defective function of a transmembrane conductance regulator protein responsible for abnormalities in the airway physiology and mucociliary clearance.¹ These pathological lung conditions are the basis of chronic infections by opportunistic microorganisms, which are the leading cause of morbidity and mortality in CF.² Many bacterial species have been identified in the CF sputum and correlated with lung disease (e.g., *Burkholderia cepacia*, *Haemophilus influenzae* or *Staphylococcus aureus*) but *Pseudomonas aeruginosa* is probably the main cause of lethality.³ *P. aeruginosa* is able to colonize lungs and develop 3D-architecture biofilms, which are very difficult to eradicate even after highly aggressive antibiotic therapies.⁴

^a Laboratorio de Nanobiomateriales, CINDEFI – Departamento de Química, Facultad de Ciencias Exactas, Universidad Nacional de La Plata – CONICET (CCT La Plata), Calles 47 y 115 (B1900AJJ) La Plata, Buenos Aires, Argentina. E-mail: grcastro@gmail.com

^b Cátedra de Control de Calidad de Medicamentos, Departamento de Ciencias Biológicas, Facultad de Ciencias Exactas, Universidad Nacional de La Plata, Calles 47 y 115 (B1900AJJ) La Plata, Buenos Aires, Argentina

^c Laboratorio de Investigación y Desarrollo de Bioactivos (LIDeB), Departamento de Ciencias Biológicas, Facultad de Ciencias Exactas, Universidad Nacional de La Plata, Calles 47 y 115 (B1900AJJ) La Plata, Buenos Aires, Argentina

^d Departamento de Química Orgánica and UMYMPOR (CONICET-UBA), Facultad de Ciencias Exactas y Naturales, Universidad de Buenos Aires, Ciudad Universitaria, Pabellón 2, Piso 3, Intendente Güiraldes 2160, C1428EGA, Buenos Aires, Argentina

† Electronic supplementary information (ESI) available: Fig. S1–S5. See DOI: 10.1039/c6tb03366k

The capability of *P. aeruginosa* to mutate into a mucoid-type strain with enhanced production of exopolysaccharide alginate, combined with high amounts of DNA from cell lysis, generates a strong bacterial biofilm niche where the bacteria can grow protected from the environment.⁵ All these elements contribute to the deterioration of lung functions in CF patients, causing airway obstruction and drastically worsen the patient's health. In this context, an early treatment of the pulmonary manifestations as well as effective antibiotic therapies is desirable to increase the life expectancy and quality of patients.^{6,7} Therefore, local administration of antibiotics directly to the lungs has become a useful alternative for the treatment of CF-associated infections.⁸ The pulmonary route of administration is advantageous compared with other routes, since the local concentration of the drug at the site of infection is high, thereby enhancing the antibacterial activity and reducing the probability of producing resistant strains. The most reliable CF therapies involve the use of tobramycin or aztreonam lysine solutions as inhalation agents to eradicate *P. aeruginosa* infections.^{9,10} However, some drawbacks have been observed, such as low drug efficacy and/or intolerance, inconveniences in drug dosing and/or reduced diffusion in the presence of the mucus accumulated in the lungs of CF patients.¹¹

Levofloxacin (LV) is a wide-spectrum antibiotic with potent activity against key pathogens, including *P. aeruginosa*; LV activity seems to be less reduced in the mucus compared with other antibiotics.¹² Additionally, LV has shown stronger antimicrobial activity than tobramycin and aztreonam in the presence of bacterial biofilms.¹³ However, oral administration of LV requires high doses to reach therapeutic levels in the lungs, which usually results in serious nephrotoxic side effects.¹⁴ It has been suggested that LV aerosols could be more effective than parenteral or oral administration, because the local lung concentrations are enough to reach the MIC (minimum inhibitory concentration) against common pathogens, avoiding higher unnecessary systemic doses.¹⁵

Many nano- and/or micro-sized drug carriers have been reported as vehicles for lung delivery of molecules from antibiotics to proteins. Some studies have reported the use of nanoparticles for lung drug delivery composed of solid lipids and cholesterol, lipid-chitosan complexes or branched synthetic polyesters that have shown high drug loadings and desirable *in vitro* release profiles.^{16–19} However, it was demonstrated that particles for lung delivery must have a diameter range from 1 μm to 5 μm for effective drug retention in the airways.²⁰ Poly(lactide-co-glycolide) (PLGA) and poly(L-lactic acid) (PLA) microparticles were developed for sustained lung release of the epinephrine analog (*i.e.*, isoproterenol) and steroid drug for asthma (*i.e.*, beclomethasone dipropionate) and they showed extended release. Besides, some disadvantages of PLGA and PLA microparticles such as tissue inflammation, increase in the neutrophil amount, hemorrhage or reduction in cell viability were reported.^{21,22} Also, the use of synthetic polymers with slow degradation rates may lead to their accumulation in the lungs, which is not beneficial for chronic pathologies (*e.g.*, cystic fibrosis, asthma) in which periodic antibiotic administration is required. In this sense, it is interesting to explore the encapsulation of LV in effective therapeutic

carriers for non-invasive local drug delivery as a potential innovative solution to CF.

Previous work from our laboratory demonstrated the effective encapsulation of LV in hybrid CaCO_3 /alginate microparticles, showing inhibitory effects against *P. aeruginosa* and suitable properties for lung delivery, but no *in vivo* experiments were performed at that moment.²³ In particular, the vaterite polymorph of calcium carbonate (CaCO_3) is the most desired crystal structure for microparticle preparation since they exhibited spherical geometry with a small crystal size, narrow distribution, and high stability.²⁴ Thus, they are attractive carriers as inert materials for pulmonary delivery since, owing to their size (around 5 μm), they can reach the deepest sites of the lungs.^{25,26} Toxicity studies in lungs indicated that calcium carbonate may cause coughing, sneezing and irritation of the nasal mucosal membranes when inhaled at excessive concentrations of pure dust. However, there are some considerations to be taken into account such as the size of the CaCO_3 powder particles and the purity grade of the raw material. The system proposed in our work is a hybrid system and the properties are highly different from the pure materials, as has been demonstrated by DRX, TGA, DSC, FTIR, and BET isotherms.^{23,27} Alginate present as a biopolymer in the formulation acts as a template for particle formation and also reduces its possible toxicity towards a more biocompatible design. In particular, alginate has been extensively proposed as a useful matrix for pulmonary delivery.²⁸ Alginates (Alg) are composed of β -mannuronic acid (M units) and α -guluronic acid (G units) linked by 1–4 bonds.²⁹ Alginates are linear anionic polysaccharides widely used in food and pharmaceutical industries due to easy gelation in the presence of divalent ions, producing non-toxic gels without immune response and high biocompatibility. Also, hybrid microparticle architectures made of CaCO_3 /Alg have the advantage of being modified by changing and tailoring the biopolymer content and the residual polymer groups on the microparticle surface using a green chemistry technology. This versatile technology allows changing the microparticle surface and porosity by using different enzyme types such as alginate hydrolases and/or alginate lyases. In particular, alginate lyase (AL) can act upon poly M, poly G or poly GM residues, cleaving the glycosidic bond through beta-elimination producing 4-deoxy-L-erythro-hex-4-ene-pyranosyluronates at the non-reducing end of alginate chains and creating “hairy” surface gel architectures that show an increased loading capacity of molecules.^{23,30}

Also, nuclease incorporation into hybrid microparticles could help in breaking down the DNA chains originated from cell lysis and accumulated in the mucus of the lungs of the CF patient. Reduction in the viscoelasticity and increase in the antibiotic diffusion across the biofilm matrix are expected to improve the antimicrobial activity of the drugs.^{31,32}

The aim of the present work was the development and biophysical characterization of an inhalable microparticulate drug delivery system based on Alg/ CaCO_3 capable of providing sustained pulmonary co-delivery of LV and DNase. Studies of DNase incorporation, activity and release from the hybrid microparticles were performed. The work also involved the

tailoring of microparticles with alginate lyase, loading analysis using a fluorescent probe, simultaneous kinetic release studies of LV and DNase, and evaluation of the antimicrobial effects against *P. aeruginosa* biofilms. The biophysical characterization of the hybrid microparticles using different spectroscopies (*i.e.*, FTIR, NMR, Z potential and XRD), microscopies (optical, epifluorescence, SEM and TEM), thermogravimetry and structural analyses (BET and BHJ) was carried out. The *in vivo* performance of the formulation was assessed in healthy mice as a pre-clinical approach.

Experimental

Reagents and cells

Levofloxacin (LV, (S)-9-fluoro-2,3-dihydro-3-methyl-10-(4-methyl-1-piperazinyl)-7-oxo-7H-pyrido[1,2,3-de]-1,4-benzoxazine-6-carboxylic acid), glycine (Gly), deoxyribonuclease (DNase) type I from bovine pancreas (MW \approx 31 kDa, pI \approx 5.2), DNase test agar with toluidine blue and alginate lyase (AL) from *Sphingobacterium multivorum* (MW \approx 39.6 kDa) were provided by Sigma-Aldrich (Buenos Aires, Argentina). Sodium alginate (MW_{av} = 120 kDa.) was purchased from Monsanto (Buenos Aires, Argentina). BSA Alexafluor[®]488 conjugate (MW \approx 67.0 kDa) was purchased from Molecular Probes (Invitrogen, Eugene, US). *Pseudomonas aeruginosa* ATCC 15442 was kindly donated by the Cathedra of Microbiology, School of Sciences, Universidad Nacional de La Plata (Argentina). Other reagents were of analytical/HPLC grade and were obtained from commercially available sources and used as received from Merck (Darmstadt, Germany) or a similar brand.

Synthesis of hybrid calcium carbonate/alginate microparticles

Hybrid microparticles (CaCO₃/Alg) were synthesized by colloidal crystallization of CaCO₃ in the presence of Gly buffer and alginate, as previously reported.²³ Briefly, 9.0 ml of an aqueous solution of Na₂CO₃ (3.2% w/v) prepared in Milli-Q water was mixed with 2.0 ml of sodium alginate solution at 1.0% w/v. Then, 9.0 ml of 3.2% w/v of CaCl₂ in Gly buffer (pH = 10.0) was added and stirred at 1000 rpm in an ice bath for 5 min. The precipitated products were collected by centrifugation at 10 000 \times g for 10 min. The resulting precipitate was washed with Milli-Q water. Later, the samples were resuspended in water, frozen in liquid N₂ and freeze-dried. Finally, the obtained light powder was stored under vacuum at room temperature until further use.

The enzymatic tailoring of the hybrid microparticle surface was performed as follows: 25.0 mg of CaCO₃/Alg microparticles was incubated with 1.5 ml of AL solution (1.0 mg ml⁻¹; 40.0 EU ml⁻¹ in 25 mM phosphate buffer, pH = 7.4) at 37 °C for 48 h. Later, the treated hybrid microparticles (named CaCO₃/Alg + AL) were washed, freeze-dried and kept as mentioned before.

Determination of degradation products of AL by nuclear magnetic resonance (NMR) analysis

The resulting soluble products from the enzymatic treatment of microparticles (CaCO₃/Alg) with AL were studied by NMR. Briefly, the products of enzymatic degradation were separated

from the microparticles by centrifugation at 10 000 \times g, and the supernatant was transferred to an ultrafiltration centrifugal device (MWCO 10 kDa, Microcon, Millipore, MA, USA) followed by centrifugation at 5000 \times g for 10 min to remove AL. The products were frozen at -80 °C and later freeze-dried. ¹H-NMR spectra were recorded at 500.13 MHz in deuterium oxide solution, on a Bruker Avance II 500 NMR spectrometer (Bruker, CA, USA). Chemical shifts are given in ppm downfield from TSP-d4 as an internal standard; J values are given in Hz.

LV and DNase loading

LV was incorporated by incubating 50.0 mg of dry microparticles in 1.0 ml of LV solution (10.0 mg ml⁻¹) at 5 °C under carousel agitation at 15 rpm for 24 h. DNase (1.0 mg ml⁻¹) was added to the solution containing the microparticles 4 hours before the incubation was stopped. After loading, the microparticles were separated by centrifugation at 10 000 \times g for 5 min and washed with Milli-Q water. The supernatant and the washing water were diluted, and LV in solution was spectrophotometrically determined at 286 nm. The maximum loading of microparticles was calculated using two methods: (a) by the difference between the amounts of drug initially dissolved into the starting solution and the LV not incorporated after the microparticle loading procedure; (b) by total dissolution of microparticles at acidic pH (1.0 M HCl), followed by UV detection of LV at 293 nm (acid pH) or 286 nm (neutral pH). The UV signal was correlated using a suitable calibration curve of LV.

The DNase encapsulation efficiency was indirectly determined by detection of the non-encapsulated enzyme in the supernatant after microparticle loading using the protocol of fluorescamine reaction (Sigma-Aldrich, EC Number 253-814-5) that specifically detected proteins. The non-fluorescent reagent reacts readily under mild conditions with primary amines in amino acids and peptides to form stable, highly fluorescent compounds. The method was used and validated in previous studies conducted in our lab.³³

Optical and epifluorescence microscopy

The mean size and distribution of wet microparticles were observed on a Leica DM 2500 microscope (Wetzlar, Germany), equipped with UV filters (495–505 nm). The ability of both CaCO₃/Alg and CaCO₃/Alg + AL microparticles to incorporate proteins by absorption and their main localization within the matrix were tested by means of their incubation with 1.0 mg ml⁻¹ BSA Alexafluor[®]488 following the previous DNase loading protocol. Microscopic observations were carried out using a green fluorescence filter at 400 \times and 1000 \times .

Additionally, epifluorescence microscopy was used to study the microparticle localization in the lungs after the *in vivo* administration of microparticles by nebulization: excised mice lungs were fixed in 10% formalin for 24 h, embedded in paraffin, and 5 μ m sections were obtained using an SM 2000R 17 Leica microtome (Wetzlar, Germany).

Scanning electron microscopy (SEM)

SEM analysis of the freeze-dried microparticles was carried out. Samples were prepared by sputtering the surface with gold

using an SCD 030 metalizer (Balzers, Liechtenstein), obtaining a layer thickness between 15 and 20 nm. The microparticle surface and morphology were observed using a Philips SEM 505 model (Rochester, USA), and processed by the SIS ADDA II digitizer program (Soft Imaging System, Lakewood, USA).

Nitrogen adsorption isotherms

Nitrogen adsorption–desorption at 77 K at a bath temperature of $-195.8\text{ }^{\circ}\text{C}$ was carried out for dry microparticles. The surface area, pore volume and pore size of the different formulations were calculated using ASAP 2020 v3.00 software (Micromeritics, USA) considering the Brunauer–Emmett–Teller (BET) equation or the Barrett–Joyner–Halenda (BJH) method.

Size distribution and roughness analysis

The microparticle average size was determined from SEM images at $500\times$ magnifications and processed using ImageJ software (NIH, USA). After setting the scale, the diameter of microparticles ($n = 100$) was measured and the mean was calculated. The roughness of the surface was reflected by the standard variation of the gray values from the pixels corresponding to each microparticle at $5000\times$ magnification. The lower the standard variation value, the smoother the surface. In this sense, histograms and plot profiles were obtained.

Differential scanning calorimetry (DSC)

The DSC profile of the samples was obtained using a TA-Instrument DSC Q2000 (DE, USA). Briefly, 5.0 mg of lyophilized powder was placed in a standard aluminum pan, hermetically closed and heated at a constant rate of $10\text{ }^{\circ}\text{C min}^{-1}$ from room temperature to $225\text{ }^{\circ}\text{C}$, at a rate of 20 ml min^{-1} of nitrogen purging. All samples were run in duplicate.

X-ray diffraction spectroscopy (XRD)

An Analytical Expert Instrument equipped with an X-ray generator ($\lambda = 0.154\text{ nm}$) was used to characterize the crystalline structure of the microparticles. Samples were scanned in the 2θ range from 2 to $50\text{ }^{\circ}\text{C}$ ($2\text{ }^{\circ}\text{C min}^{-1}$).

Fourier transform infrared spectroscopy (FTIR)

The FTIR spectra of the lyophilized samples were directly recorded on a Thermo Scientific Nicolet 6700 spectrometer, at a resolution of 4 cm^{-1} . 32 scans were performed for each sample in the range $600\text{--}4000\text{ cm}^{-1}$. The ATR (attenuated total reflectance) accessory was utilized to perform all measurements as a tool to preserve the microparticle integrity. The rough data were smoothed using SigmaPlot software to attenuate background noise.

In vitro release of LV and DNase from microparticles

Loaded microparticles (25.0 mg) were incubated in 1.0 ml of physiological solution (pH = 7.0) at $37\text{ }^{\circ}\text{C}$ for 72 h. Samples were centrifuged at different times, and 500 μl was withdrawn. The drug release was followed by UV detection at the maximum wavelength of LV (286 nm) and by the fluorescamine method for DNase. To keep the volume constant, samples were refilled

with fresh media, simulating the dynamic conditions during pulmonary drug delivery.

Determination of DNase activity

The activity of DNase after release from microparticles was determined in agar medium (DNase agar test). A volume of 50 μl of the supernatant after 72 h release was seeded on an agar plate and incubated at $37\text{ }^{\circ}\text{C}$ for 24 h. The appearance of a violet halo around the seed in a blue plate background indicates the enzymatic hydrolysis of DNA.

Microbiological assays

Inhibition haloes against *P. aeruginosa* were determined by using the modified disk diffusion method according to international clinical standards (CLSI/NCCLS), replacing disks for sterile glass cylinders (8 mm \times 6 mm \times 10 mm of external and internal diameters, and length, respectively). The glass cylinders were further placed on the agar plate surface inoculated with bacteria (0.5 McFarland scale). The supernatants (50 μl), after release of LV from microparticles for 72 h, were placed inside the cylinders and incubated at $37\text{ }^{\circ}\text{C}$ for 24 h. Then, inhibition zones were measured.

Staining biofilms using the Live/Dead BacLight[®] kit

The kit is composed of two fluorescent dyes, SYTO9[®] (green) and propidium iodide (red), able to determine intact microbial cells and membrane-damaged and/or dead ones, respectively. For the microbiological assays, *P. aeruginosa* cells growing at the late exponential phase were inoculated in soft nutrient agar (1 : 10 dilution) and then, a microbial drop of 20 μl was placed on the surface of a glass slide, followed by incubation for 24 h to allow biofilm formation. Subsequently, the biofilm was covered with a suspension of $\text{CaCO}_3/\text{Alg} + \text{AL}$ microparticles (containing LV and DNase) for 30 and 60 min. After treatment, the biofilms were carefully washed with deionized water. For biofilm staining, a mixture of both dyes was prepared in equal proportions (0.75 μl of each dye in 0.5 ml of sterile deionized water), applied onto the entire biofilm and held in the dark for 20 min. Then, the samples were washed using deionized water and observed on a Leica DM 2500 epifluorescence microscope (Wetzlar, Germany) equipped with UV filters (495–505 nm) to determine the viability of the bacteria. The filters used were U-MWG2 (excitation between 510 and 550 nm and emission at 590 nm) to observe live bacteria (green) and U-MWB2 (excitation at 460 nm and emission at 490–520 nm) for damaged and/or dead bacteria (red).

Transmission electron microscopy (TEM)

The *P. aeruginosa* growing at an exponential phase before and after treatment with loaded microparticles for 24 h were washed in physiological solution, and a drop of the dispersion was spread onto a collodion-coated Cu grid (400-mesh). The excess liquid was drained using filter paper. Finally, TEM analysis was performed using a Jeol-1200 EX II-TEM microscope (MA, USA).

In vivo testing of microparticles

Swiss mice provided by the School of Veterinary Sciences, National University of La Plata, weighing between 18 and 23 g at the time of testing, were used as experimental animals. Mice were housed in colony cages under a 12 h light/dark cycle and provided with food and water *ad libitum*. Prior to the experiments, the animals were individually acclimated for 30 min per day for four days in restraint tubes.

For pulmonary administration of the microparticles, two methodologies were assayed: nebulization and dry powder inhalation. For nebulization, a compressor nebulizer system, Aspen NA 182 (Multiflow, Argentina) was used. Each animal received the microparticles suspended in 5.0 ml of physiological solution *via* a homemade whole-body inhalation exposure chamber, for an exposure time of 20 min (Fig. S1, ESI[†]). The upstream of the chamber was connected to the nebulizer (and sealed with Parafilm[®]), and the downstream of the chamber was open to air through a distal hole to maintain a continuous air flow through the whole system. Prior to the experiments, the animals were individually acclimated for 30 min per day for four days in falcon tubes. On the other hand, for the dry powder inhalation method the mice were exposed to the powder in a nose-only manner using the method reported by Kaur *et al.* (Fig. S2, ESI[†]).³⁴

Mice were divided into groups of $N = 5$ and, for the preclinical PK study, a total of eight groups were used. One group was subjected to the dry powder inhalation method and four groups were used for the comparison of the CaCO₃/Alg microparticles *vs.* the free drug (as a solution) *via* the nebulization method at two different doses: 0.7 mg (dose 1) and 1.4 mg (dose 2) of LV. Three more groups were needed to study the LV lung concentration at 120 min post-administration of CaCO₃/Alg microparticles, as well as CaCO₃/Alg + AL microparticles at 0 and 120 min post-dose. Finally, an additional group of two mice were used for the study of the microparticle distribution in the lungs by epifluorescence microscopy.

After treatment, mice were euthanized by cervical dislocation, and lungs were harvested and rinsed twice with physiological solution. Tissues were frozen until further analysis.

Animal experiments were performed in compliance with the relevant laws and institutional guidelines of the Institutional Committee on Care and Use of Experimental Animals (CICUAL) of the Facultad de Ciencias Exactas (Universidad Nacional de La Plata, Argentina) that has approved all the experiments.

All experiments were performed in compliance with the relevant laws and institutional guidelines. The Institutional Committee on Care and Use of Experimental Animals (CICUAL) from the School of Sciences, University of La Plata, Argentina, has granted approval for all the experiments involving laboratory animals reported in this article.

Quantification of LV levels in mouse lung tissue

Frozen mouse lung tissue was cut into pieces and placed in 2.0 ml of a mixture of acetonitrile and 10% trifluoroacetic acid (70:30), previously spiked with 14 μ l of the internal standard

solution (IS, stock solution of enrofloxacin 450 μ g ml⁻¹ in methanol). The samples were placed in an ice bath for their mechanical homogenization, and then centrifuged for 15 min at 3500 rpm. Two 0.9 ml aliquots were taken from the supernatant and extracted twice with 2 ml of dichloromethane. For each sample, the combined organic phases were evaporated to dryness.

Quantification was performed on a Dionex Ultimate 3000 UHPLC (Thermo Scientific, CA, USA) configured using a dual gradient tertiary pump (DGP-3000) and a DAD-3000 diode array detector. The stationary phase was a Luna RP-18 column (150 \times 4.6 mm, 5 μ m, Phenomenex, USA) and the mobile phase was a 67:33 mixture of methanol and 20 mM KH₂PO₄ buffer adjusted to pH = 2.5 with phosphoric acid. The system was operated isocratically at a flow rate of 1 ml min⁻¹, and the detection was performed at 300 nm. The samples were dissolved in 100 μ l of mobile phase and centrifuged (15 000 \times g for 5 min at 4 $^{\circ}$ C) prior to injection (20 μ l).

In order to validate the method, samples were prepared in blank homogenized lung tissue by the addition of known concentrations of free LV, microparticle-encapsulated LV and IS. The response was linear in the range 0.02 (LQ)–15.00 μ g ml⁻¹. In all cases, precision RSD values were lower than 4.0%, recovery was around 70%, and accuracy was between 90% and 100%. The method was specific to the biological matrix, and the drugs (LV and IS) proved to be stable in both the methanolic solution (stock solutions) and the biological matrix.

Statistical analysis

Experiments were carried out with a minimum of 3 replications. The number of replications, when more than three were done, is specified in the corresponding section. According to the number of groups to be compared, comparisons of the means were performed by Student's *t*-test or by analysis of variance (ANOVA, followed by Tukey's HSD test). A significance level of 0.05 was used.

For the preclinical PK studies, groups of $N = 5$ animals were used since five is the minimum number of animals which, according to our previous data of standard deviation (SD) \approx 0.1 μ g mg⁻¹, allows for the detection of statistically significant differences in LV concentration of around 0.2 μ g mg⁻¹ with the desired power of 0.8 (Student's *t*-test, non-paired data).

Results and discussion

Preparation and observation of hybrid microparticles

CaCO₃/Alg microparticles were prepared by the co-precipitation method and treated with AL to increase their porosity.²³ The resulting enzymatic products were purified and analyzed by ¹H-NMR spectroscopy in order to confirm the substrate specificity of AL over the alginate chains from the surface (Fig. S3, ESI[†]). The characteristic peaks of the alginate structure were observed at 4.69–4.63 ppm (internal signals of β -D-mannuronate units) and 5.04–4.45 ppm (internal signal of α -L-guluronate units) in concordance with previous reports.³⁵ The presence of G and M reducing end signals (in the range of 4.90–4.86 ppm)

Table 1 Co-encapsulation efficiency of LV and DNase into the microparticles

Microparticles	LV		DNase	
	LE ^a	MDM ^b	LE ^a	MDM ^b
CaCO ₃ /Alg	21.1 ± 0.8%	42.1	28.7 ± 3.4	11.5
CaCO ₃ /Alg + AL	37.4 ± 1.8%	74.8	67.8 ± 2.2	27.1

^a LE: loading efficiency (%). ^b MDM: mass drug/mass matrix ($\mu\text{g mg}^{-1}$).

overlapped with the HOD signal of the solvent. However, these results suggested the enzymatic cleavage of the alginate bonds to produce small fragments detected in the supernatant of the reaction.³⁶

The mean diameter of the produced wet microparticles was observed by optical microscopy, indicating the presence of spherical microparticles with diameters in the range of 3–5 μm in a narrow size distribution with optimum properties for pulmonary delivery (Fig. S4, ESI†).

Loading of microparticles with LV and DNase

The incorporation of LV into the hybrid microparticles was based on a previous protocol developed in our laboratory²³ with two modifications: (1) the concentration of LV in the loading medium was increased ten times (10.0 mg ml^{-1}) in order to increase the drug/matrix ratio; and (2) DNase was absorbed after 4 hour incubation to increase the therapeutic potential of microparticles with a mucolytic component.³¹ The results are summarized in Table 1.

Based on the previous results, hybrid CaCO₃/Alg microparticles were able to load 4.3 μg of LV per mg of matrix, but in the present work we have demonstrated that the drug loading could be increased about ten times higher than the one previously reported.²³ This is an advantageous approach since a lower amount of administered carrier is required to reach antibiotic therapeutic levels in the lungs.

This load increase could be explained not only by the rise of the concentration gradient, but also by the aromatic ring (π - π) stacking phenomena commonly described for fluoroquinolones at high concentrations.³⁷ On the other hand, AL treated CaCO₃/Alg microparticles exhibited higher drug loading efficiency, almost two-times higher compared with the untreated microparticles, mainly due to the increase in the specific surface area and porosity of the microparticles after enzymatic treatment.²³

The loading capacity of DNase into microparticles was also evaluated and the results listed in Table 1 showed that CaCO₃/Alg microparticles were able to load 29% of the initial enzyme amount, while in CaCO₃/Alg + AL microparticles the amount was more than double (68%). Considering the molecular weight of DNase (about 31 kDa) and its globular structure,³⁸ protein dimensions around 37.5 nm^3 with a mean diameter of 4.2 nm were estimated by using the equation previously reported by Erickson (2009).³⁹ Taking into account this calculation and that CaCO₃/Alg microparticles have a pore diameter of about 6 nm (determined by the nitrogen isotherm adsorption technique) it was possible to establish that the

enzyme could hardly penetrate into the core of the microparticles, and the mechanism can be described mainly as an adsorption phenomenon (*i.e.* on the matrix surface). On the other hand, CaCO₃/Alg + AL microparticles exhibited a pore diameter of 13 nm and it was expected that DNase would not only be adsorbed onto the surface but could also penetrate inside the core of microparticles, which possibly explains the increase in the DNase loading efficiency.

In order to confirm the statement that CaCO₃/Alg microparticles mainly incorporate the enzyme onto their surface, whereas CaCO₃/Alg + AL microparticles show a deeper interpenetration of DNase, experiments with fluorescence-labeled BSA (with about two times the MW of DNase) were carried out (Fig. 1). The microscopy images showed that CaCO₃/Alg microparticles were indeed able to incorporate the labeled BSA (Fig. 1a and b). The inset in Fig. 1b clearly demonstrates that the fluorescence was mainly distributed on the surface of the microparticles.

In contrast, CaCO₃/Alg + AL microparticles displayed higher fluorescence than CaCO₃/Alg ones. In fact, the exposure time of the microscope camera was reduced ten times to obtain the microphotographs because the higher amount of fluorescence in the samples saturated the signal. Also, CaCO₃/Alg + AL microparticles exhibited a different distribution pattern of fluorescence, which was observed not only on the surface of the microparticles but also in the core, suggesting deep penetration of the protein into the particles (Fig. 1c and d). These results are coherent considering that the microparticle average pore diameter is around 13 nm and the estimated dimensions of BSA are approximately $7.5 \times 6.5 \times 4.0 \text{ nm}$.³⁹ The estimated volumes of the pore matrix (calculated as a half-sphere located on the matrix surface) and BSA were about 575.2 nm^3 and 195.0 nm^3 , respectively. Consequently, the ratio between the matrix and BSA is roughly 3 times, suggesting that BSA is able to diffuse inside the hybrid microspheres.

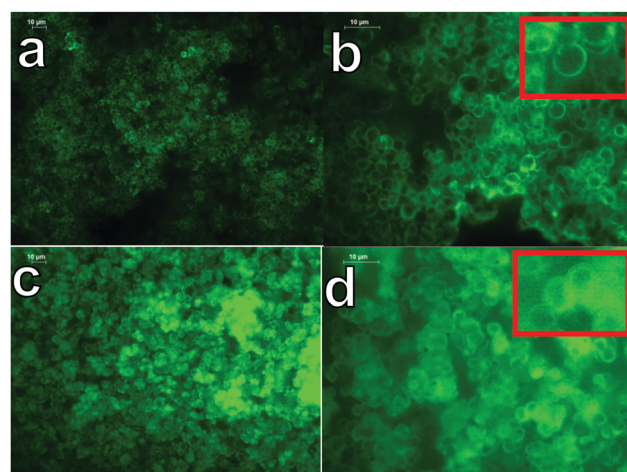


Fig. 1 Epifluorescence microscopy images after absorption of AlexaFluor BSA into CaCO₃/Alg (a and b) and CaCO₃/Alg + AL treated (c and d) microparticles at 400 and 1000 \times magnification. The exposition time of the microscope was 20 millis for CaCO₃/Alg and 2 millis for CaCO₃/Alg + AL treated microparticles.

Physicochemical characterization of loaded microparticles

The freeze-drying process of hybrid microparticles produced the fine homogenous powders displayed in the SEM images, which provide information about the size, shape and distribution of the microparticles (Fig. 2). The presence of some non-representative aggregates could be observed in samples due to the absence of cryoprotectants extreme drying experimental conditions.⁴⁰ CaCO₃/Alg hybrid microparticles did not show considerable differences in size distribution before and after DNase and LV loading (Fig. 2a–d). Surface analysis using ImageJ software indicated a similar distribution of the gray scale in empty and loaded microparticles with a standard deviation of 24.4 and 24.9, respectively (inset in Fig. 2b and d, respectively).

Furthermore, the particles maintained their spherical shape after loading. However, strong differences were found on the CaCO₃/Alg + AL microparticle surface. The loading of DNase

and LV was evidenced by the filling of the pores, which smoothed the typical rough surface of empty microparticles (Fig. 2e–h). The surface analysis revealed a decrease of 30% in the roughness after drug loading (the standard deviation value switched from 31.1 to 20.9) suggesting the presence of DNase covering the surface of the microparticles. In all cases, the microparticle size distribution is in the range of 3–5 μm, which is the average size recommended for effective lung delivery.²⁶

Nitrogen adsorption isotherms of hybrid CaCO₃/Alg + AL microparticles loaded and unloaded with LV/DNase were measured to confirm the SEM observations (Fig. 3).

The surface area of CaCO₃/Alg + AL microparticles calculated by using the BET (Brunauer–Emmett–Teller) equation was 75 m² g⁻¹ and 30 m² g⁻¹ for empty and LV/DNase loaded matrices, respectively. The 1.5 times decrease in the surface area can be explained considering the absorption of DNase by the microparticles. In fact, DNase absorption reduces the pore size diameter from 13 nm to 10 nm. As previously estimated, the mean diameter of DNase was around 4 nm, suggesting its incorporation into the matrix by filling the calcium carbonate pores through a diffusional mechanism. Furthermore, in both cases a tensile strength effect (TSE) was observed, which is produced by the sudden liquid–gas transition of nitrogen. The TSE phenomenon suggests the presence

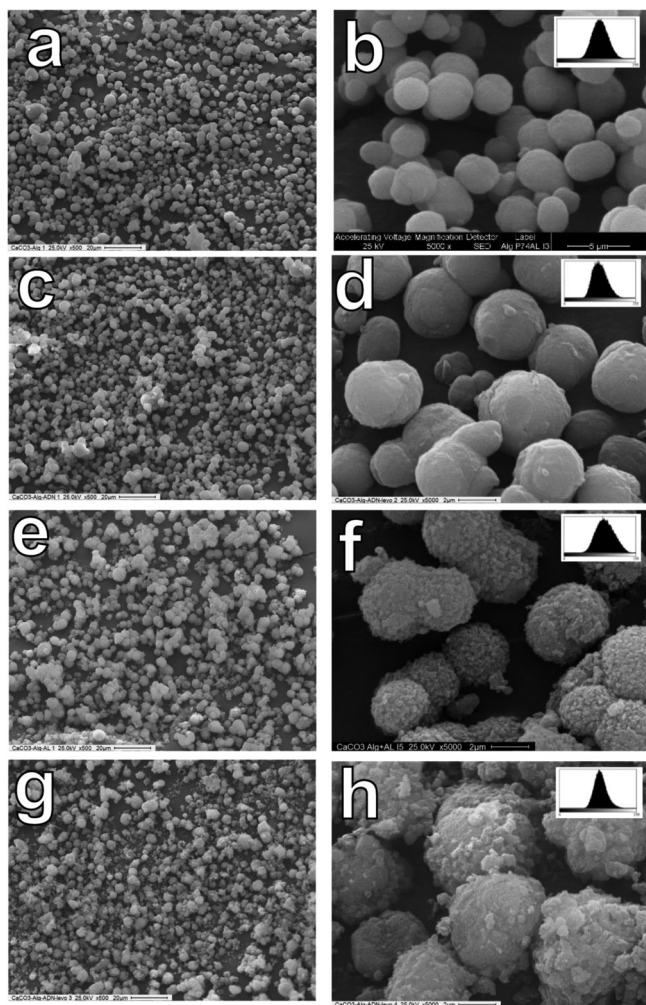


Fig. 2 SEM images of microparticles at 500× and 5000× magnifications: CaCO₃/Alg empty (a and b) and loaded with LV and DNase (c and d); CaCO₃/Alg + AL empty (e and f) and loaded with LV and DNase (g and h). The insets show the histogram distribution of the microparticle surface analyzed by using ImageJ software.

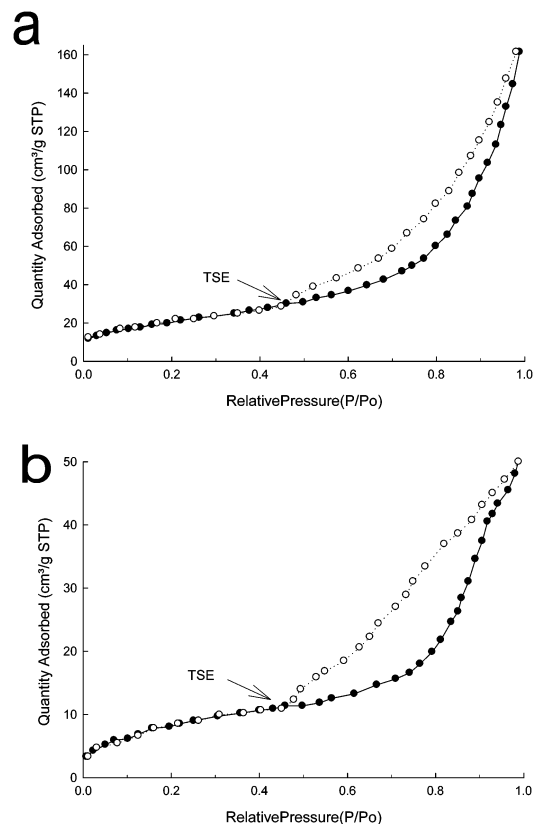


Fig. 3 Nitrogen adsorption–desorption isotherms of CaCO₃/Alg + AL treated microparticles: empty (a) and LV/DNase loaded (b). Adsorption (●) and desorption (○) isotherms. TSE: tensile strength effect.

of pore networks and occurs when interconnected larger pores have to empty the nitrogen through pores with a smaller diameter.⁴¹ These results are interesting since they show the effect of LV/DNase loading into the hybrid microparticles, keeping the macroporous and mesoporous structures inside the hybrid microparticles undisturbed.

The effect of the load on the hybrid $\text{CaCO}_3/\text{Alg} + \text{AL}$ microparticles was also analyzed by Z potential measurements and the results revealed changes in hybrid microspheres after loading (Fig. S5, ESI[†]). Empty microparticles exhibited negative values around -20 mV, mainly due to the presence of deprotonated carboxylic groups from alginate. On the other side, the Z potential of LV/DNase loaded $\text{CaCO}_3/\text{Alg} + \text{AL}$ microparticles decreased by 15% (to more positive values) and could be explained by the steric coating of DNase on the microparticle surface. In addition, the same tendency was observed in the mobility values, which reflect the ability of a charged particle to move across an electric field.

The DSC profile allows establishing the thermal characterization of loads and microparticles (Fig. 4).

The thermograms of LV and DNase displayed endothermic peaks at 43 °C and 44 °C, respectively. These melting peaks were not observed in the DSC profile of loaded microparticles (with LV and with LV/DNase), suggesting a good dispersion of loads in an amorphous state into the calcium carbonate matrix. Furthermore, the shift of the endothermic peak of $\text{CaCO}_3/\text{Alg} + \text{AL}$ microparticles to higher temperatures after loading the cargo molecules could indicate the stabilization of the matrix by internal non-covalent interactions with the loads.

The vibrational spectra of the cargo molecules and loaded microparticles were analyzed by ATR-FTIR, and the results are displayed in Fig. 5. LV showed typical vibrational bands of the carbonyl ($\text{C}=\text{O}$ stretching vibration at 1730 cm^{-1}), the amine ($\text{C}-\text{N}$ stretching at 1294 cm^{-1}) and the fluorine ($\text{C}-\text{F}$ stretching at 1080 cm^{-1}) groups present in the molecule.⁴² The free DNase displayed typical bands of the protein amide I and II bands at 1641 cm^{-1} and 1535 cm^{-1} , respectively. Peaks at 1736 cm^{-1} and

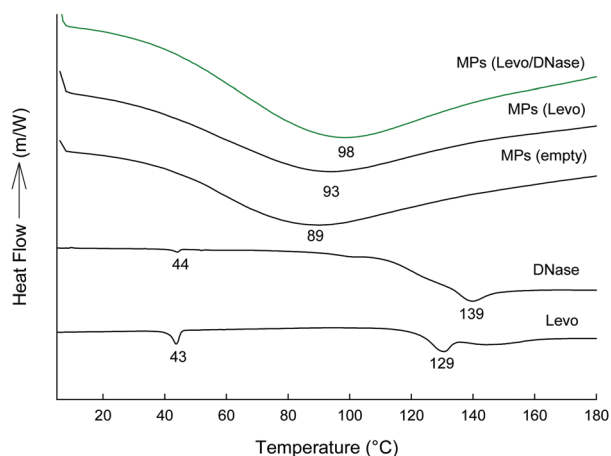


Fig. 4 DSC thermograms of levofloxacin, DNase, $\text{CaCO}_3/\text{Alg} + \text{AL}$ treated microparticles (MPs) empty, loaded with LV and co-loaded with LV and DNase.

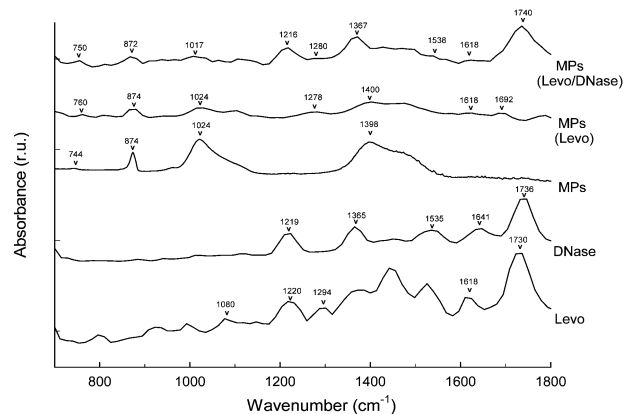


Fig. 5 ATR-FTIR spectra of levofloxacin, DNase, and empty, loaded with LV and co-loaded with LV/DNase $\text{CaCO}_3/\text{Alg} + \text{AL}$ microparticles.

1219 cm^{-1} could be assigned to the $\text{C}=\text{O}$ and $\text{C}-\text{N}$ vibration modes.⁴³ The band at 1642 cm^{-1} could also suggest a random coil conformation of DNase.⁴⁴ The spectra of hybrid calcium carbonate microparticles showed a weak peak associated with the polymorph structure of vaterite at 744 cm^{-1} and, on the other hand, an intense peak at 1024 cm^{-1} probably associated with the degradation products of alginate after enzymatic hydrolysis.^{23,30}

In microparticles loaded with LV, the peaks of the CaCO_3 structure were observed, and some of them with short shifts towards higher frequencies. However, it was interesting to see the appearance of new peaks associated with LV at 1692 cm^{-1} , 1618 cm^{-1} and 1278 cm^{-1} , which indicates the presence of the drug inside the matrix. Finally, in the $\text{CaCO}_3/\text{Alg} + \text{AL}$ microparticles loaded with LV and DNase, some bands associated with the calcium carbonate structure were observed (1017 cm^{-1} , 874 cm^{-1} and 750 cm^{-1}) with slight shifts mainly due to weak interactions with the loads. Also, bands related to the LV structure at 1618 cm^{-1} and 1280 cm^{-1} were observed. It was noticed that the spectrum is dominated by the presence of DNase peaks (1740 cm^{-1} , 1538 cm^{-1} , 1367 cm^{-1} and 1216 cm^{-1}), which confirms the presence of the enzyme on the microparticle surface (Fig. 2g and h).

In order to gain new structural insights into the microparticles, X-ray diffraction patterns were recorded (Fig. 6). LV showed intense peaks at $2\theta = 6.61^\circ$, 9.69° , 13.05° , 15.75° , 19.45° , 26.35° , 31.49° and 45.37° , in agreement with previous reports.⁴⁵ The DNase pattern was not clear under the present experimental conditions, probably owing to the amorphous state of the enzyme, but it showed a wide peak with a maximum at $2\theta = 20.0^\circ$. Regarding the matrix, typical peaks of the CaCO_3 vaterite polymorph at $2\theta = 25^\circ$ and 33° were observed. In addition, the diffraction patterns did not show the most intense peak of the calcite polymorph located at $2\theta = 29.3^\circ$. This result is advantageous since vaterite crystals are more stable and can probably be attributed to the presence of alginate acting as a template for microparticles.²³ No peaks associated with the loads were observed in the XRD patterns of $\text{CaCO}_3/\text{Alg} + \text{AL}$ microparticles containing LV and DNase/LV, suggesting that

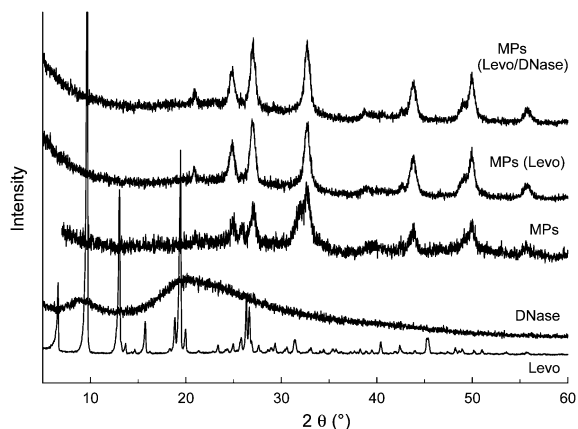


Fig. 6 XRD diffractograms of levofloxacin, DNase, and empty, loaded with LV and co-loaded with LV and DNase CaCO_3/Alg + AL treated microparticles.

the antibiotic and the enzyme could be molecularly dispersed within the matrix in an amorphous state.

In vitro release experiments from microparticles

The *in vitro* release profile of LV and DNase from hybrid microparticles was measured in physiological solution at pH 7.0 followed by the corresponding biological tests of the supernatant (bactericidal and DNase activity tests, respectively) (Fig. 7). Particularly, the DNase agar test has the advantage of detecting enzymatic activity against gelled substrates and under similar physiological conditions found in the lungs of CF patients.

The kinetics of DNase and LV release showed two main phases: burst load release up to 6 h, which was attributed to the DNase and LV on the surface and initial swelling of the microparticles. The second phase was extended release, in which the loads entrapped inside the microparticles may be released by a diffusional mechanism plus microparticle degradation. LV controlled release kinetics from CaCO_3/Alg and CaCO_3/Alg + AL microspheres were observed (Fig. 7a).

At 72 h, the CaCO_3/Alg microparticles released nearly 45% of the total antibiotic content, while CaCO_3/Alg + AL microparticles released only 35% at the same time. This decrease of LV release

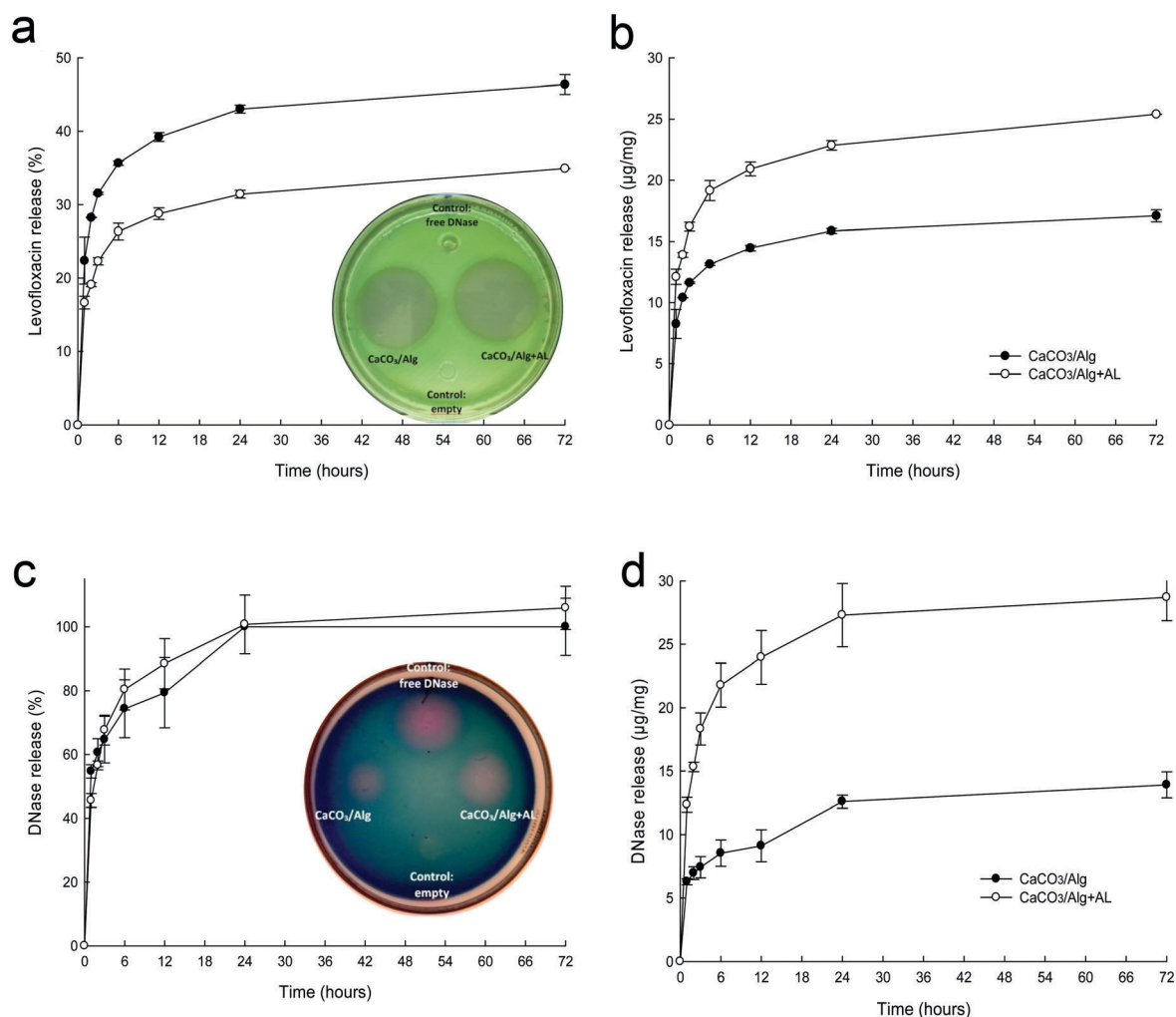


Fig. 7 *In vitro* release profile of LV (a and b) and DNase (c and d) from CaCO_3/Alg and CaCO_3/Alg + AL microparticles. The release is expressed as percentage (%) or mass of drug per mass of matrix ($\mu\text{g mg}^{-1}$). The insets show the LV and DNase activities from the supernatants at 72 h release (controls: free DNase and empty microparticles). LV is tested against *P. aeruginosa* ATCC 15442.

in the AL treated microparticles could be attributed to the dense layer of DNase covering the surface, which may act as a diffusional barrier for the LV release from the core of the matrix to the bulk solution. However, the total amount of LV release was almost twice for CaCO₃/Alg + AL microparticles compared to the untreated ones, which is consistent with the higher loads achieved by the AL treatment (Fig. 7b).

The supernatant of the microparticle medium after the 72 h release experiment was tested in agar plates against *P. aeruginosa* (inset in Fig. 7a). Inhibition haloes of the bacteria clearly indicated that LV had been released in its active form from the microparticles. Negative controls with DNase and the supernatant of empty microparticles were tested to show the absence of antimicrobial activity.

On the other hand, the DNase release profiles from CaCO₃/Alg and CaCO₃/Alg + AL microparticles were very similar, showing a complete release of the enzyme in about 24 h (Fig. 7c and d). The results suggest that DNase desorption from the carriers follows a similar kinetics, dissolving the most exposed layers from the surface into the bulk solution. This is a relevant result considering the weak interactions between the enzyme and the matrix that allow the DNase to be completely released from the matrix before the total release of LV, thus facilitating the antibiotic ability to reach its microbial target. Also, it confirms the hypothesis that DNase was in a non-crystalline state (amorphous) as previously demonstrated, taking into account that drugs in the amorphous state tend to dissolve more easily than in the crystalline form (Fig. 4 and 6). The study of the mass of DNase released per mass of microparticles after 72 h revealed that treated microparticles are capable of delivering more than double the amount of enzyme in comparison with untreated ones: 29 ± 2 and $14 \pm 1 \mu\text{g mg}^{-1}$, respectively (Fig. 7d). In agreement with these results, the DNase activity in the supernatant of the release media was evaluated, showing that the CaCO₃/Alg + AL microparticles exhibited a higher DNase activity related to the halo diameter compared to the untreated hybrid microparticles (inset in Fig. 7c). The fact that DNase is released in 24 h and faster than LV becomes interesting since it could be expected that the enzyme firstly will act on the dense mucus accumulated in the lungs of CF patients, thus enhancing the subsequent diffusion of the antibiotic to kill the microorganisms.^{32,46} The release profiles of both components possibly followed a charge-mediated phenomenon.⁴⁷ At the neutral pH of the release medium, LV is mainly in its zwitterionic form (isoelectric point 6.77) considering the two pK_a values of 5.59 (carboxylic acid) and 7.94 (protonation of the piperazinyl group).⁴⁸ On the other hand, DNase showed a mean isoelectric point in the range of 4.8–5.2 (provided by Sigma), the reason why it was expected to be negatively charged.⁴⁰ The microparticle matrix containing alginate chains was mainly negatively charged according to Fig. S5 (ESI[†]), possibly due to the deprotonation of carboxylic groups from alginate (pK_a in the range 3.4–4.0).²⁹ Below those considerations an electrostatic repulsion of the DNase from the microparticles was expected, which explains its faster release than LV.

Antimicrobial activity of microparticles

The antimicrobial activity of LV/DNase loaded CaCO₃/Alg + AL microparticles was tested against *P. aeruginosa*, the most common pathogen associated with CF. The time dependence of viability after treatment was established using the Live/Dead BacLight[®] kit (Fig. 8a). Untreated bacteria were able to produce a biofilm after 24 h of incubation, and a high amount of living bacteria was observed in green. By covering the biofilm surface with a suspension of microparticles (2.0 mg ml^{-1}), red zones began to appear after a 30 min incubation period due to the presence of damaged cells. All of the bacteria on the biofilm were killed one hour later. Similar results were previously reported by our group with a lipidic nanosystem.⁴⁵ However, an extended residence time in the lung tissue with reduced macrophage uptake is expected with these hybrid microparticles considering that the average size of the carrier is around $5.0 \mu\text{m}$.^{25,26}

TEM observations corroborated the bactericidal capability of CaCO₃/Alg + AL microparticles. While living *Pseudomonas* cells showed membrane integrity and maintained their typical bacillus shape, the bacteria treated with a suspension of microparticles for 24 h exhibited membrane rupture and cellular debris due to bacterial lysis (Fig. 8b and c). These results highlight the importance of the developed device as an alternative to effectively eradicate *P. aeruginosa* from a CF patient's lungs.

Determination of microparticle distribution in lung tissue by epifluorescence microscopy

In the first *in vivo* experimental approach, healthy animals were treated with microparticles to know whether the encapsulated drug has better localization in the lungs than in the free drug.

Mice were nebulized with a suspension of microparticles (8.0 mg ml^{-1}) in physiological solution and after sacrifice, the lungs were extracted and prepared for observation using epifluorescence microscopy, considering that loaded microparticles showed the typical LV fluorescence (Fig. 9).

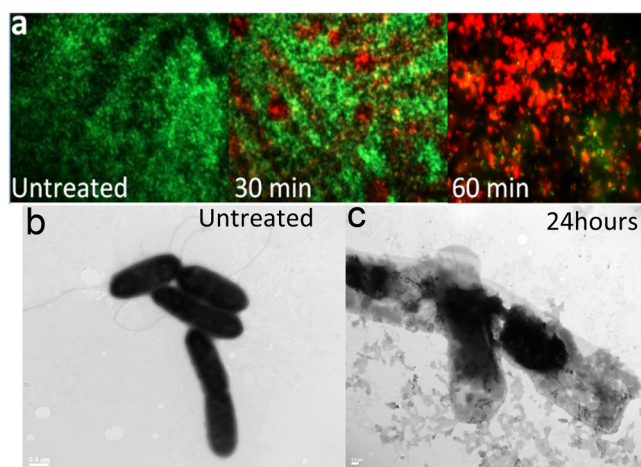


Fig. 8 Antimicrobial assays of microparticles against *Pseudomonas aeruginosa* determined by using the Live/Dead BacLight[®] kit (a) and by TEM observations (b and c).

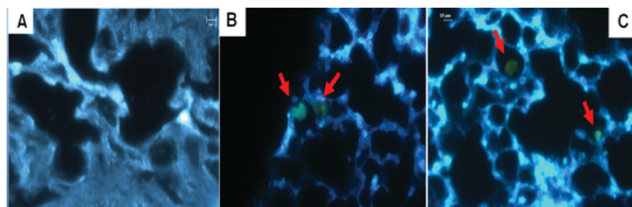


Fig. 9 Epifluorescence microscopy of mice lungs after administration of loaded microparticles. (a) Untreated; (b and c) treated by nebulization. Arrows show the location of microparticles.

However, normal lung tissue presented autofluorescence, which is the reason why LV-loaded microparticles were observed with green fluorescence. Microparticles seem to be located along the respiratory tract, but it was interesting to observe the presence of microparticles at the alveolus site, suggesting a good penetration after nebulization.

Preclinical pharmacokinetic study

Mice were subjected to the pulmonary administration of LV at two different doses: 0.7 and 1.4 mg LV (dose 1 and 2, respectively), both as free drug solution and encapsulated into CaCO₃/Alg and CaCO₃/Alg + AL microparticles (Fig. 10A).

Previously, it was found that the administration of hybrid microparticles *via* the nebulization technique (microparticles resuspended in physiological solution) or *via* dry powder inhalation showed pulmonary LV levels of 0.8 ± 0.3 and $0.7 \pm 0.5 \mu\text{g g}^{-1}$ of tissue (mean of $N = 5 \pm \text{SD}$), respectively, which were not statistically different ($p \geq 0.05$). However, the nebulization technique was selected for further assays considering better reproducibility (37% of relative SD against 90% for the dry powder inhalation). The administration of LV loaded into microparticles showed a great difference compared with the administration of the same dose as free drug (Fig. 10A). At dose 1 (0.7 mg LV, equivalent to 20 mg CaCO₃/Alg LV-loaded microparticles) the amount of LV detected in the lungs was 7.4 times higher for the microparticulate formulation compared to the LV in solution ($p = 0.001$). Meanwhile, at dose 2 (1.4 mg LV, equivalent to 40 mg

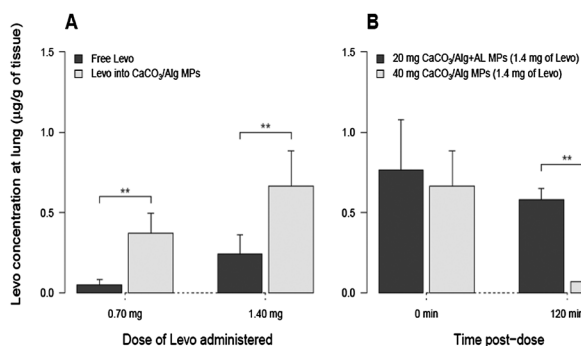


Fig. 10 LV levels in mice lung tissue quantified by HPLC after administration of: (A) LV as free solution and encapsulated into CaCO₃/Alg microparticles, at two doses and; (B) LV loaded CaCO₃/Alg and CaCO₃/Alg + AL microparticles (1.4 mg of LV) at different times. The mean of $N = (5 + \text{SD})$ is presented.

of CaCO₃/Alg LV loaded microparticles) microparticles yielded lung levels 2.8 times higher than that of the free drug ($p = 0.008$). The considerable increase of LV concentrations in the lungs by the administration of hybrid microparticles could be explained taking into account that microparticles increase the residence time of the drug in the lungs by avoiding the loss of the drug along the respiratory tract.⁴⁹

Regarding the PK behavior of untreated LV-loaded (CaCO₃/Alg) vs. treated (CaCO₃/Alg + AL) microparticles, significant differences in the concentration vs. time profile were also found. After the administration of LV at dose 2 (equivalent to 40 mg of CaCO₃/Alg to 20 mg of CaCO₃/Alg + AL) no significant differences were observed at zero time, suggesting that both types of microparticles are able to reach the same lung interstices. However, 2 h post-dose CaCO₃/Alg + AL microparticles showed pulmonary LV concentrations 8.9 times higher compared with untreated microparticles ($p = 0.0001$) (Fig. 10B). These results are consistent with the previous *in vitro* LV release profiles, where slower release kinetics were evidenced in the case of the enzymatically treated microparticles (Fig. 7).

Conclusions

In the present work, a hybrid microparticulate carrier composed of alginate and CaCO₃ enzymatically modified with alginate lyase was prepared and then loaded with LV and DNase. The resulting microparticles have an average diameter of 5 μm, thus being a promising therapeutic system for the pulmonary delivery of their cargoes. Studies with a fluorescent protein probe demonstrated the capability of macromolecules such as DNase to diffuse inside the microparticles treated with AL and be released in a controlled profile. The enzymatic partial degradation of the alginate on the microparticle surface increases the microparticle porosity, enhancing the loading capacity by almost two times for LV and more than twice for DNase.

The biophysical characterization of the hybrid microparticles demonstrated the presence of vaterite as a crystal component of the hybrid microparticles, as well as spherical morphology and a good diameter distribution range for lung drug delivery. Furthermore, the presence of LV and DNase very well dispersed in the hybrid matrix, with non-covalent interactions between the loads and the matrix components, could be confirmed.

In vitro release experiments of LV and DNase followed by TEM observation and microbiological studies showed high activity of the microparticles against *P. aeruginosa* biofilms, along with high enzymatic activity in the DNase agar test, indicating that the enzyme is released from the microparticles in its active form.

In vivo studies demonstrated the high efficiency of the hybrid microparticle formulation to reach the mice lungs, attaining higher levels of LV in comparison with the administration of the free antibiotic. They also suggested a slow release of the drug at the site of action/infection for at least 2 h post-dose in the case

of AL treated particles. It is interesting to note that the kinetics of drug release and absorption seems to be highly dependent on the surface treatment of the microparticles.

Therefore, the CaCO₃/Alg + AL microparticles containing LV and DNase presented here are a promising drug delivery system for the treatment of the CF disorder, since they are able to reach the lungs and release their cargoes with a dual kinetics: a fast release of the DNase content followed by a sustained release of LV. Altogether, these results indicate their potentiality to reduce the viscoelasticity of the mucus layers that act as the main diffusional barrier protecting *P. aeruginosa* colonies against strong antibiotic treatments. Finally, the experimental results show the effectiveness of microparticles for improving the antibiotic bioavailability in the lungs. In this sense, we expect to carry out new experiments using a CF-animal model that could allow establishing clinically relevant outcomes for improving the treatment of CF in the near future.

Acknowledgements

The present work was supported by Argentine grants from CONICET (National Council for Science and Technology, PIP 0498), The National Agency of Scientific and Technological Promotion (ANPCyT, PICT 2011–2116), and Fundación Argentina de Nanotecnología, UNLP (National University of La Plata, 11/X545 and PRH 5.2) to GRC. Also, GAI wants to thank the “Grant for Young Researchers from UNLP 2013” and “Premio a la Innovación UNLP 2014” for financing some reagents used in the present work. We also appreciate some data provided by Dr Pablo Cortez Tornello (Cindefi, Argentina), Ms Sofia Goicoechea and Mr Sebastian Scioli Montoto (LIDeB, Argentina).

Notes and references

- 1 G. R. Cutting, *Nat. Rev. Genet.*, 2015, **16**, 45–56.
- 2 D. L. Longo, D. a Stoltz, D. K. Meyerholz and M. J. Welsh, *N. Engl. J. Med.*, 2015, **372**, 351–362.
- 3 A. Folkesson, L. Jelsbak, L. Yang, H. K. Johansen, O. Ciofu, N. Høiby and S. Molin, *Nat. Rev. Microbiol.*, 2012, **10**, 841–851.
- 4 O. Ciofu, L. F. Mandsberg, H. Wang and N. Høiby, *FEMS Immunol. Med. Microbiol.*, 2012, **65**, 215–225.
- 5 M. I. Lethem, S. L. James, C. Marriott and J. F. Burke, *Eur. Respir. J.: Off. J. Eur. Soc. Clin. Respir. Physiol.*, 1990, **3**, 19–23.
- 6 F. Ratjen, G. Döring and W. H. Nikolaizik, *Lancet*, 2001, **358**, 983–984.
- 7 R. L. Gibson, J. Emerson, N. Mayer-Hamblett, J. L. Burns, S. McNamara, F. J. Accurso, M. W. Konstan, B. A. Chatfield, G. Retsch-Bogart, D. A. Waltz, J. Acton, P. Zeitlin, P. Hiatt, R. Moss, J. Williams and B. W. Ramsey, *Pediatr. Pulmonol.*, 2007, **42**, 610–623.
- 8 K. C. Kesser and D. E. Geller, *Respir. Care*, 2009, **54**, 754–767.
- 9 L. M. Rose and R. Neale, *Sci. Transl. Med.*, 2010, **2**, 63mr4.
- 10 K. a Pesaturo, E. R. Horton and P. Belliveau, *Ann. Pharmacother.*, 2012, **46**, 1076–1085.
- 11 G. Doring, P. Flume, H. Heijerman and J. S. Elborn, *J. Cystic Fibrosis*, 2012, **11**, 461–479.
- 12 V. R. Anderson and C. M. Perry, *Drugs*, 2008, **68**, 535–565.
- 13 D. E. Geller, P. A. Flume, D. C. Griffith, E. Morgan, D. White, J. S. Loutit and M. N. Dudley, *Antimicrob. Agents Chemother.*, 2011, **55**, 2636–2640.
- 14 C. Carbon, *Chemotherapy*, 2001, vol. 47, pp. 9–14.
- 15 G. Döring and A. Dalhoff, *Expert Opin. Orphan Drugs*, 2013, **1**, 549–556.
- 16 A. Grenha, C. Remuñán-López, E. L. S. Carvalho and B. Seijo, *Eur. J. Pharm. Biopharm.*, 2008, **69**, 83–93.
- 17 J. Liu, T. Gong, H. Fu, C. Wang, X. Wang, Q. Chen, Q. Zhang, Q. He and Z. Zhang, *Int. J. Pharm.*, 2008, **356**, 333–344.
- 18 M. Beck-Broichsitter, J. Gauss, C. B. Packhaeuser, K. Lahnstein, T. Schmehl, W. Seeger, T. Kissel and T. Gessler, *Int. J. Pharm.*, 2009, **367**, 169–178.
- 19 J. Varshosaz, S. Ghaffari, S. F. Mirshojaei, A. Jafarian, F. Atyabi, F. Kobarfard and S. Azarmi, *BioMed Res. Int.*, 2013, **2013**, 136859.
- 20 M. Y. Yang, J. G. Y. Chan and H. K. Chan, *J. Controlled Release*, 2014, **193**, 228–240.
- 21 D. J. Armstrong, P. N. Elliott, J. L. Ford, D. Gadsdon, G. P. McCarthy, C. Rostron and M. D. Worsley, *J. Pharm. Pharmacol.*, 1996, **48**, 258–262.
- 22 R. H. Müller, S. Maaßen, H. Weyhers, F. Specht and J. S. Lucks, *Int. J. Pharm.*, 1996, **138**, 85–94.
- 23 G. A. Islan, M. L. Cacicedo, V. E. Bosio and G. R. Castro, *J. Colloid Interface Sci.*, 2015, **439**, 76–87.
- 24 T. Beuquier, B. Calvignac, G. J.-R. Delcroix, M. K. Tran, S. Kodjikian, N. Delorme, J.-F. Bardeau, A. Gibaud and F. Boury, *J. Mater. Chem.*, 2011, **21**, 9757.
- 25 F. Ishikawa, M. Murano, M. Hiraishi, T. Yamaguchi, I. Tamai and A. Tsuji, *Pharm. Res.*, 2002, **19**, 1097–1104.
- 26 S. Haruta, T. Hanafusa, H. Fukase, H. Miyajima and T. Oki, *Diabetes Technol. Ther.*, 2003, **5**, 1–9.
- 27 V. E. Bosio, M. L. Cacicedo, B. Calvignac, I. León, T. Beuquier, F. Boury and G. R. Castro, *Colloids Surf., B*, 2014, **123**, 158–169.
- 28 S. Alipour, H. Montaseri and M. Tafaghodi, *Colloids Surf., B*, 2010, **81**, 521–529.
- 29 S. K. Bajpai and S. Sharma, *React. Funct. Polym.*, 2004, **59**, 129–140.
- 30 G. A. Islan, C. Dini, L. C. Bartel, A. D. Bolzán and G. R. Castro, *Int. J. Pharm.*, 2015, **496**, 953–964.
- 31 F. Ratjen, K. Paul, S. Van Koningsbruggen, S. Breitenstein, E. Rietschel and W. Nikolaizik, *Pediatr. Pulmonol.*, 2005, **39**, 1–4.
- 32 M. Alipour, Z. E. Suntres and A. Omri, *J. Antimicrob. Chemother.*, 2009, **64**, 317–325.
- 33 G. A. Islan, V. E. Bosio and G. R. Castro, *Macromol. Biosci.*, 2013, **13**, 1238–1248.
- 34 J. Kaur, P. Muttill, R. K. Verma, K. Kumar, A. B. Yadav, R. Sharma and A. Misra, *Eur. J. Pharm. Sci.*, 2008, **34**, 56–65.
- 35 K. A. M. Natania, P. Y. Jung, L. E. E. E. Yeol and K. I. M. H. Sook, *Can. J. Microbiol.*, 2004, **50**, 1032–1041.

- 36 T. Y. Wong, L. A. Preston and N. L. Schiller, *Annu. Rev. Microbiol.*, 2000, **54**, 289–340.
- 37 N. Maurer, K. F. Wong, M. J. Hope and P. R. Cullis, *Biochim. Biophys. Acta, Biomembr.*, 1998, **1374**, 9–20.
- 38 W.-J. Chen and T.-H. Liao, *Protein Pept. Lett.*, 2006, **13**, 447–453.
- 39 H. P. Erickson, *Biol. Proced. Online*, 2009, **11**, 32–51.
- 40 W. Abdelwahed, G. Degobert, S. Stainmesse and H. Fessi, *Adv. Drug Delivery Rev.*, 2006, **58**, 1688–1713.
- 41 J. C. Groen, L. A. A. Peffer and J. Pérez-Ramírez, *Microporous Mesoporous Mater.*, 2003, **60**, 1–17.
- 42 S. Gunasekaran, K. Rajalakshmi and S. Kumaresan, *Spectrochim. Acta, Part A*, 2013, **112**, 351–363.
- 43 H. Tajmir-Riahi, C. N'soukpoe-Kosi and D. Joly, *Spectroscopy*, 2009, **23**, 81–101.
- 44 W. Kabsch, H. G. Mannherz, D. Suck, E. F. Pai and K. C. Holmes, *Nature*, 1990, **347**, 37–44.
- 45 G. A. Islan, P. C. Tornello, G. A. Abraham, N. Duran and G. R. Castro, *Colloids Surf., B*, 2016, **143**, 168–176.
- 46 J. J. T. M. Swartjes, T. Das, S. Sharifi, G. Subbiahdoss, P. K. Sharma, B. P. Krom, H. J. Busscher and H. C. Van Der Mei, *Adv. Funct. Mater.*, 2013, **23**, 2843–2849.
- 47 B. A. Tepy, R. Tong, S. Y. Jeong, G. Luther, I. Sherifi, C. H. Yim, A. Khademhosseini, O. C. Farokhzad, R. S. Langer and J. Cheng, *Biomaterials*, 2008, **29**, 1216–1223.
- 48 I. Ahmad, R. Bano, M. A. Sheraz, S. Ahmed, T. Mirza and S. A. Ansari, *Acta Pharm.*, 2013, **63**, 223–229.
- 49 J. Fiegel, J. Fu and J. Hanes, *J. Controlled Release*, 2004, **96**, 411–423.